

Microstructure of Al-Zn-Mg-Cu-Zr-0.5Er alloy under as-cast and homogenization conditions

WANG Shao-hua¹, MENG Ling-gang¹, YANG Shou-jie²,
FANG Can-feng¹, HAO Hai¹, DAI Sheng-long², ZHANG Xing-guo¹

1. School of Materials Science and Engineering, Dalian University of Technology, Dalian 116024, China;

2. Beijing Institute of Aeronautical Materials, Beijing 100095, China

Received 26 August 2010; accepted 6 April 2011

Abstract: The billets of Al-Zn-Mg-Cu-Zr and Al-Zn-Mg-Cu-Zr-0.5Er alloys were prepared by semi-continuous direct chill casting (DCC). The effects of trace Er on microstructure of Al-Zn-Mg-Cu-Zr alloy under as-cast and homogenization conditions were studied. The results show that the grain morphology is large dendritic structure and the grain size increases obviously by the addition of 0.5% Er. Moreover, most of Er element in the alloy segregates at grain boundary during solidification, resulting in ternary $\text{Al}_8\text{Cu}_4\text{Er}$ phase. After homogenization, most of the MgZn_2 phase at grain boundary has dissolved back to Al matrix in the two alloys. In the Er-containing alloy, the dissolution temperature of $\text{Al}_8\text{Cu}_4\text{Er}$ phase is about 575 °C. Therefore, the homogenization treatment cannot eliminate $\text{Al}_8\text{Cu}_4\text{Er}$ phase validity.

Key words: Al-Zn-Mg-Cu-Zr alloy; Er; $\text{Al}_8\text{Cu}_4\text{Er}$ phase; homogenization; microstructure

1 Introduction

With the rapid development of aerospace and military industries, mechanical properties of Al-Zn-Mg-Cu alloys are required to be further improved to satisfy the applications. The requirement is from single high strength to high strength and toughness and good stress corrosion cracking (SCC) resistance [1–2]. To achieve these aims, microalloying with transition or rare earth elements, such as scandium (Sc), zirconium (Zr) [3–5] and erbium (Er) [6], is proved to be an effective method.

It is well accepted that trace additions of rare earth elements are of great importance to improve the microstructure and mechanical properties of aluminum alloys. Sc has been studied mostly as beneficial microalloying element due to the presence of elastically hard, coherent and nano-sized Al_3Sc (Li_2) particles, which strongly refine as-cast grain size and inhibit the dynamic recrystallization and dislocation movement. Furthermore, combined additions of Sc and Zr are shown to be more effective in refining as-cast grain size and

improving mechanical properties because of the newly formed $\text{Al}_3(\text{Sc}, \text{Zr})$ particles in the Al-Zn-Mg-Cu alloys [7–8]. However, the applications of Sc-containing alloys are extremely restricted due to the high cost of Sc addition. Therefore, more attention is focused on rare earth Er, which is much cheaper than Sc.

In Al-Zn-Mg [6] and Al-Mg [9] alloys, trace Er can improve the strength and refine grain size due to the formation of fine dispersed Al_3Er precipitates. Addition of Er in Al-4%Cu series alloys, Er atoms may segregate at grain boundary during solidification, resulting in ternary $\text{Al}_8\text{Cu}_4\text{Er}$ phase [10–13]. However, the influence of trace Er on Al-Zn-Mg-Cu-Zr alloy is few in previous literatures [14–15].

In this study, the billets of Al-Zn-Mg-Cu-Zr and Al-Zn-Mg-Cu-Zr-0.5Er alloys were prepared by semi-continuous direct chill casting (DCC). The present work mainly aims at investigating the influence of Er on microstructure of the alloy under as-cast and homogenization conditions. The study on mechanical properties of the alloys will be reported in a separate paper.

Foundation item: Project (50875031) supported by the National Natural Science Foundation of China; Project (2005CB623705) supported by National Basic Research Program of China

Corresponding author: ZHANG Xing-guo; Tel: +86-411-84706183; E-mail: zxgwj@dlut.edu.cn

DOI: 10.1016/S1003-6326(11)60880-7

2 Experimental

The chemical compositions of alloys are provided in Table 1. The base alloy, named alloy 1, was prepared using commercial pure Al and Mg, and Al-50%Cu and Al-5%Zr master alloys. The other alloy with 0.5% Er addition, named alloy 2, was prepared using an addition of Al-10%Er master alloy. The $\phi 126$ mm-billets were prepared by conventional DCC process, which melt temperature was $(720 \pm 10)^\circ\text{C}$ with a casting speed of 120 mm/min. After casting process, the billets were homogenized at 400°C for 12 h plus at 470°C for 36 h.

The samples were obtained at the 1/2 radius in the transverse section from the billets. The microstructure of the alloys were characterized using electron backscatter diffractometer (EBSD), X-ray diffractometer (XRD), scanning electron microscope (SEM) and energy dispersive X-ray spectroscopy (EDS). In addition, differential thermal analysis (DTA) was used to analyze the transition of phases during the homogenization treatment. Local chemical compositions and the distributions of alloy elements were determined by electron probe microanalysis (EPMA).

Table 1 Chemical composition of experiment alloys (mass fraction, %)

Alloy No.	Zn	Mg	Cu	Zr	Er	Si	Fe	Al
1	7.55	1.68	1.53	0.11	—	0.014	0.012	Bal.
2	7.53	1.40	1.57	0.11	0.50	0.012	0.013	Bal.

3 Results

3.1 Grain structure

Figure 1 presents the orientation imaging maps of the as-cast alloys 1 and 2 using EBSD technology, respectively. The orientation imaging map can show morphology and size of alloys more clearly than the ordinary optical micrograph. The typical grain structure of as-cast alloy 1 is shown in Fig. 1(a). It consists of nearly equiaxed grains with continuous eutectic phases at the grain boundary. The grain size of the casting is about $50\ \mu\text{m}$. However, with the addition of 0.5% Er, there is obvious change in the grain structure throughout alloy 2. The cast structure of alloy 2 is predominated by large dendritic structure, and the average grain size increases to about $130\ \mu\text{m}$, as shown in Fig. 1(b). The grain sizes along the radius direction in the transverse section of alloy 2 are non-homogeneous, with large dendritic structure ($150\ \mu\text{m}$) around the center and nearly equiaxed grains ($50\ \mu\text{m}$) in the side.

3.2 Phase constitution

Figure 2 shows the X-ray diffraction (XRD)

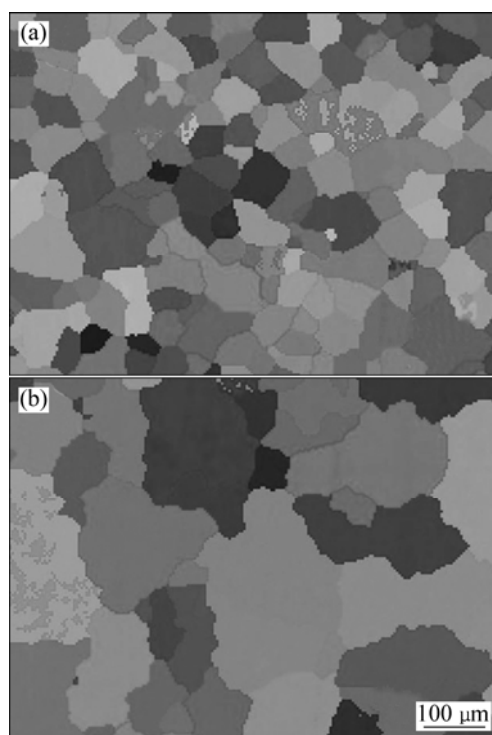


Fig. 1 EBSD graphs of alloys: (a) As-cast alloy 1; (b) As-cast alloy 2

patterns of alloy 1 and alloy 2. It can be observed that as-cast alloy 1 is mainly composed of $\alpha(\text{Al})$ solid solution and MgZn_2 secondary phase. After homogenization of alloy 1, there are no obvious diffraction peaks of secondary phases else except for $\alpha(\text{Al})$. This indicates that MgZn_2 phase, which was formed during the solidification process, has dissolved back to Al matrix. The diffusion velocity of Cu is lower than that of Zn or Mg, which results in the most difficult to dissolve in Al-Zn-Mg-Cu alloy during homogenization. Therefore, the dissolution quantity of Cu is an important factor to investigate the homogenization technology. Figure 3 shows the backscattered electron image (BEI) and element mapping of Cu in alloy 1 after

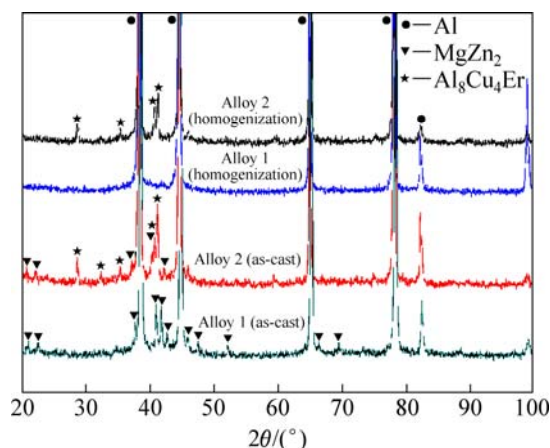


Fig. 2 XRD patterns of alloys

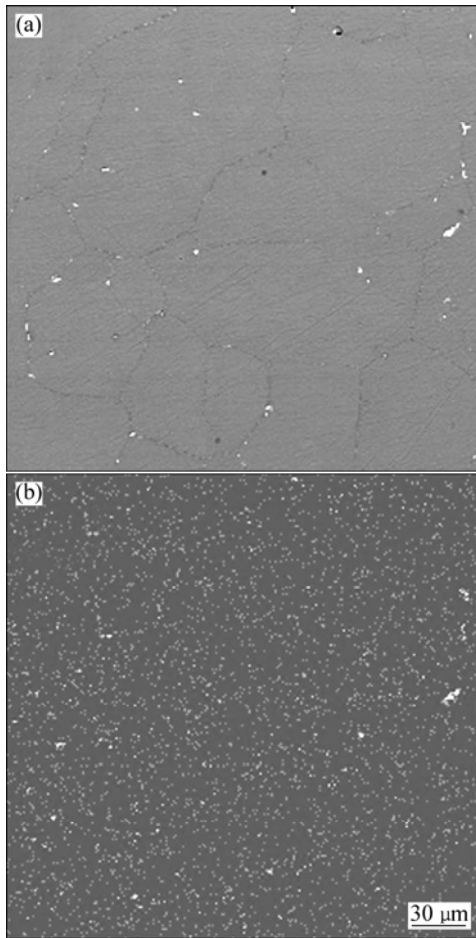


Fig. 3 BEI (a) and Cu element mapping analysis (b) of homogenized alloy 1

homogenization. It reveals that most of the eutectic structure and Cu at grain boundaries have dissolved back to Al matrix.

Besides the two phases mentioned above, a new $\text{Al}_8\text{Cu}_4\text{Er}$ phase is observed in the XRD result of as-cast alloy 2, as shown in Fig. 2. Meanwhile, many bright particles with size in the range of 1–10 μm are clearly observed in the grain boundary eutectic structure of as-cast alloy 2, as shown in Fig. 4(a). The EDS analysis reveals these particles to be different with interdendritic eutectic structure (Table 2). The gray interdendritic eutectic structure, marked A, can be identified as MgZn_2 phase. However, the EDS result of MgZn_2 indicates that more Cu and Al exist in the phase. In spite of more contribution of Al, matrix may be involved in the EDS signal of the MgZn_2 because of its small size. It is obvious that the MgZn_2 dissolves Cu and Al elements to form $\text{Mg}(\text{Zn},\text{Cu},\text{Al})_2$ phase [16]. The bright particles, marked B in Fig. 4(a), are identified as $\text{Al}_8\text{Cu}_4\text{Er}$ phases based on the results of EDS analysis (Table 2) and XRD pattern (Fig. 2).

After homogenization for alloy 2, the diffraction

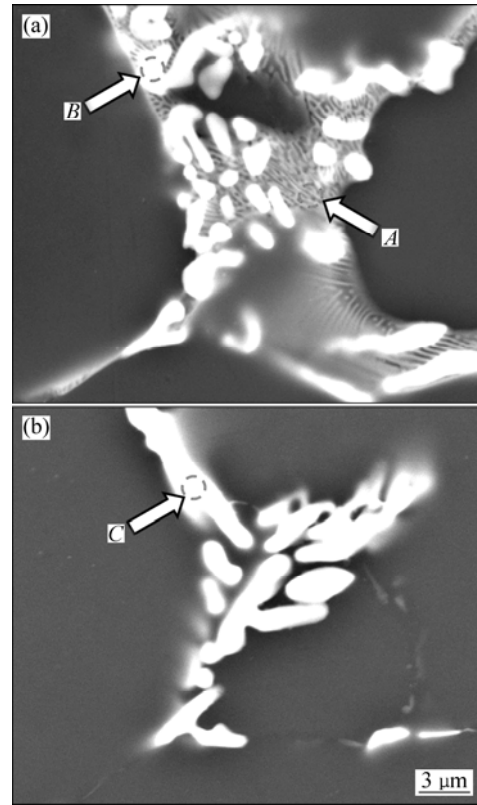


Fig. 4 SEM images at grain boundary of as-cast (a) and homogenized (b) alloy 2

Table 2 Compound compositions at grain boundary of alloy 2 in Fig. 4 (mole fraction, %)

Item	Cu	Mg	Zn	Er	Al
A	7.04	17.41	23.89	0.77	50.89
B	19.09	—	11.53	4.72	64.67
C	17.92	—	5.21	4.09	72.78

peaks of MgZn_2 phase disappear. However, the diffraction peaks of $\text{Al}_8\text{Cu}_4\text{Er}$ phase still can be observed clearly, as shown in Fig. 2. Figure 4(b) illustrates the SEM image at grain boundary of alloy 2 after homogenization. Compared with Fig. 4(a), there are still many bright particles at grain boundary. Whereas, the interdendritic eutectic structure along the grain boundary has dissolved back to the Al matrix, which accords to the XRD results shown in Fig. 2. Chemical composition of the bright particles shown in Fig. 4(b), marked C, is given in Table 2. They are identified as $\text{Al}_8\text{Cu}_4\text{Er}$ phases through the former discussion in this study. It can be also found that Zn content dissolved in $\text{Al}_8\text{Cu}_4\text{Er}$ phase is lower than that under as-cast condition. Figure 5 presents the BEI and elements mapping of Cu and Er in alloy 2 after homogenization. It indicates that elements Cu and Er still aggregate at grain boundary in the form of $\text{Al}_8\text{Cu}_4\text{Er}$ phase during this stage.

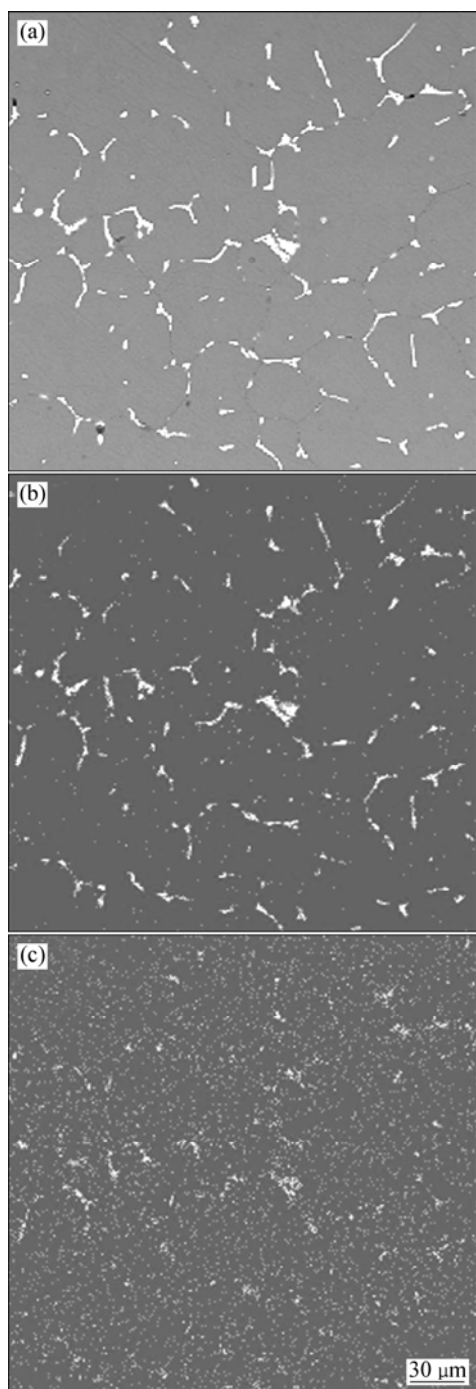


Fig. 5 BEI (a) and elements Cu (b) and Er (c) mapping analyses of homogenized alloy 2

4 Discussion

4.1 As-cast microstructure

In the Al-Zn-Mg-Cu alloy, $\eta(\text{MgZn}_2)$ phase is thought to be the predominant phase under as-cast condition. However, other phases may be observed, such as $\text{S}(\text{Al}_2\text{CuMg})$, $\text{T}(\text{Al}_2\text{Mg}_3\text{Zn}_3)$ and $\theta(\text{Al}_2\text{Cu})$. It depends on the chemical composition of the alloy and non-equilibrium freezing process [16].

The MgZn_2 phase is the main phase in alloy 1, which distributes along grain boundary. It is in correspondence with the XRD result, as shown in Fig. 2. In the alloy 2, the grain is of large dendritic structure with the size of almost three times larger than alloy 1, as shown in Fig. 1. Moreover, a new phase, i.e. $\text{Al}_8\text{Cu}_4\text{Er}$, is found at grain boundary (Fig. 4(a)).

When 0.5% Er is added to the base alloy, there is not Al_3Er phase but $\text{Al}_8\text{Cu}_4\text{Er}$ phase in the alloy 2. This phase distributes along grain boundaries, which can not be used for heterogeneous nucleation. Thus, more alloying elements aggregate ahead of the moving solid/liquid interface, and the amount of heterogeneous nucleation decreases during solidification. Due to the non-homogeneous of solute and temperature field in the melt, the size of grain increases by the pattern of dendritic structure.

In order to investigate the formation mechanism of $\text{Al}_8\text{Cu}_4\text{Er}$ phase, the DTA curves of alloy 1 and alloy 2 under different conditions are tested, as shown in Fig. 6. The scan from as-cast alloy 1 shows only one distinct endothermic peak at the temperature of about 474 °C (in this study, the endothermic peak of Al melting point at 638 °C is not considered). The reaction corresponding to the peak is the dissolution reaction of low melting eutectic compound (MgZn_2 phase). The DTA curve of as-cast alloy 2 presents two clear endothermic peaks, one happens at temperature of about 474 °C and the other at about 575 °C, as shown in Fig. 6. The former peak at 474 °C can be identified as the same from alloy 1, i.e. the dissolution reaction of MgZn_2 phase. What need to further study is the latter endothermic peak at about 575 °C, which has been marked by rectangle in Fig. 6. There is few research or similar report about this peak. However, associated with the results of XRD (Fig. 2) and SEM observation (Fig. 4(a)), the peak can be presumed as the dissolution reaction of $\text{Al}_8\text{Cu}_4\text{Er}$ phase provisionally.

In order to verify the reliability of the presumption,

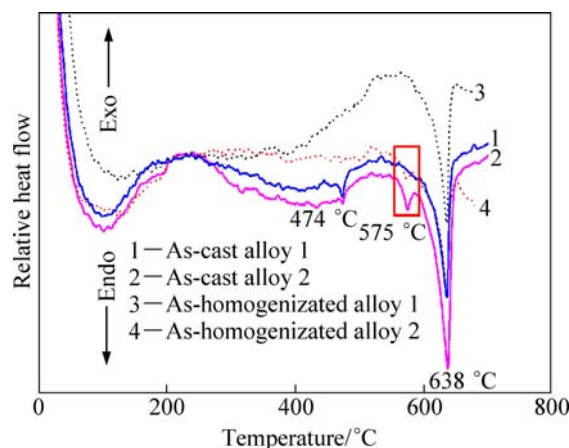


Fig. 6 DTA curves of alloys

another experiment was carried out. Two samples of as-cast alloy 2 were obtained, and one was held at 570 °C for 20 min (570 °C, 20 min) and the other was held at 580 °C for the same time (580 °C, 20 min). SEM images and EDS analysis at grain boundary of two samples are shown in Fig. 7. After holding at 570 °C for 20 min for alloy 2, there are also many bright particles along grain boundary, as shown in Fig. 7(a). The EDS analysis reveals that the particles are $\text{Al}_8\text{Cu}_4\text{Er}$ phases, which is inserted in Fig. 7(a). It indicates that the temperature of 570 °C is not high enough to dissolve $\text{Al}_8\text{Cu}_4\text{Er}$ phase back to Al matrix. However, there is distinct change along grain boundary when the holding temperature increases to 580 °C, as shown in Fig. 7(b). The overburnt feature can be seen clearly along grain boundary, and new interdendritic eutectic structure can be found clearly instead of bright particles. The EDS analysis inserted in Fig. 7(b) shows that the eutectic structure consists of lots of Al and Cu elements and a small amount of Er, Mg and Zn elements. The results illuminate that the $\text{Al}_8\text{Cu}_4\text{Er}$ phase has melted at 580 °C. Meanwhile, the interdendritic eutectic structure is the result of reaction between melted $\text{Al}_8\text{Cu}_4\text{Er}$ phase and Al matrix near grain boundary. Therefore, 575 °C is the dissolution temperature of $\text{Al}_8\text{Cu}_4\text{Er}$ phase (Fig. 6), which is in the

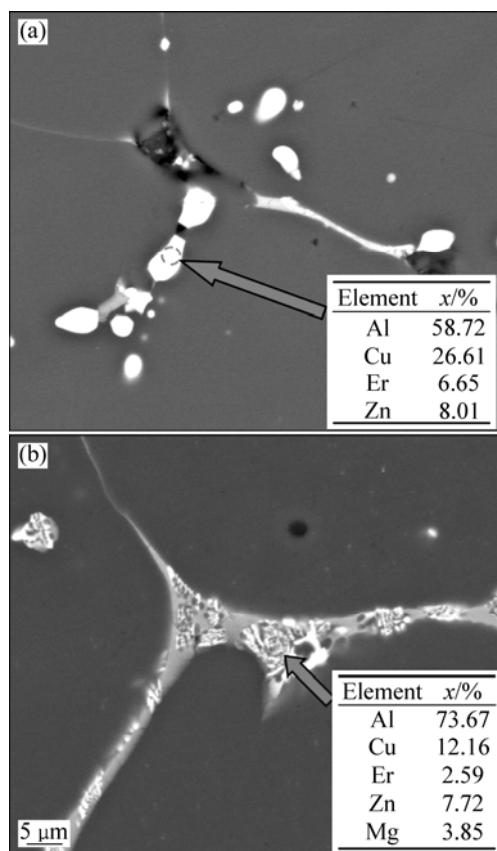


Fig. 7 SEM image and EDS analysis at grain boundary of as-cast alloy 2 under different conditions: (a) At 570 °C for 20 min; (b) At 580 °C for 20 min

range of 570–580 °C.

Accordingly, the formation of $\text{Al}_8\text{Cu}_4\text{Er}$ phase in alloy 2 during the solidification process can be described simply and cursorily below, as shown in Fig. 8. The solubility of Er is small at room temperature in aluminum alloys [10]. Even though prepared by DCC technology, most of Er is rejected ahead of the moving solid/liquid interface during solidification. The content of Er in the non-solidified grain boundary is high, and only a small amount of Er dissolves to the Al matrix. Meanwhile, the high concentrations of Cu, Mg and Zn aggregate in this region too (Fig. 8(b)). When the temperature decreases to a higher temperature (maybe about 575 °C), $\text{Al}_8\text{Cu}_4\text{Er}$ phases nucleate in grain boundary region firstly (Fig. 8(c)). Then, with decreasing the temperature to a lower temperature (maybe about 474 °C), a large amount of interdendritic eutectic compounds (MgZn_2 phases) are formed gradually (Fig. 8(d)). Therefore, the addition of 0.5% Er does not play a role in promoting nucleation or refining as-cast microstructure, but promotes the formation of $\text{Al}_8\text{Cu}_4\text{Er}$ phase at grain boundary.

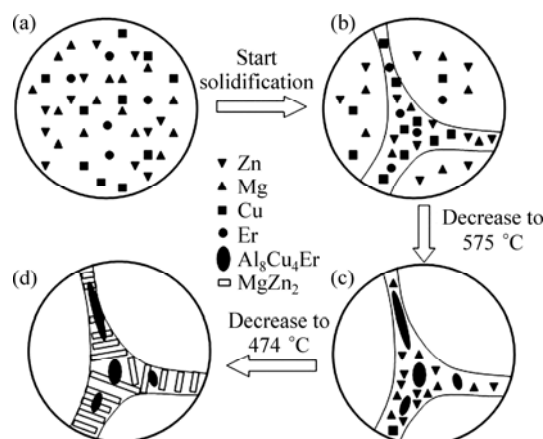


Fig. 8 Schematic diagrams of formation of $\text{Al}_8\text{Cu}_4\text{Er}$ phase in alloy 2 during solidification

4.2 Homogenization microstructure

The main purpose of homogenization is to dissolve the coarse interdendritic eutectic compound formed during solidification in Al-Zn-Mg-Cu alloys. In this investigation, MgZn_2 in alloy 1 dissolves back to Al matrix almost completely after homogenization. However, the $\text{Al}_8\text{Cu}_4\text{Er}$ phase still exists in alloy 2 after homogenization, as shown in Fig. 2 and Fig. 4(b). The DTA curves of alloy 1 and alloy 2 after homogenization are presented in Fig. 6. No obvious peaks except Al melting point can be found after homogenization in alloy 1, whereas, the peak at 575 °C also exists in alloy 2. The alloys were treated at 400 °C for 12 h plus 470 °C for 36 h, which is close to the dissolution temperature of MgZn_2 phase (474 °C), therefore, the MgZn_2 phase almost

dissolves back to Al matrix both in alloy 1 and alloy 2. However, the homogenization temperature (470 °C) is far from the dissolution temperature of $\text{Al}_8\text{Cu}_4\text{Er}$ phase (575 °C). Thus, many $\text{Al}_8\text{Cu}_4\text{Er}$ phases still distribute at grain boundary after homogenization, as shown in Fig. 4(b).

5 Conclusions

1) The grain morphology is of large dendritic structure, and grain size increases obviously with the addition of 0.5% Er to the alloy. Moreover, most of Er element in the alloy segregates at grain boundary during solidification, resulting in ternary $\text{Al}_8\text{Cu}_4\text{Er}$ phase.

2) After homogenization, most of the MgZn_2 phase at grain boundary has dissolved back to Al matrix in the two studied alloys. In the Er-containing alloy, the dissolution temperature of $\text{Al}_8\text{Cu}_4\text{Er}$ phase is about 575 °C. Therefore, the homogenization treatment in this study cannot eliminate $\text{Al}_8\text{Cu}_4\text{Er}$ phase availably.

References

- [1] CHEN Chang-qi. Development of ultrahigh-strength aluminum alloy [J]. Chinese Journal of Nonferrous Metals, 2002, 12(S1): 22-27. (in Chinese)
- [2] WANG Hong-bin, HUANG Jin-feng, YANG Bin, ZHANG Ji-shan, ZHANG Yong-an, XIONG Bai-qing. Research status and development of super-strength Al-Zn-Mg-Cu alloy [J]. Mater Res, 2003, 17(9): 1-4. (in Chinese)
- [3] ROKHLIN L L, DOBATEKINA T V, BOCHVAR N R, LYSOVA E V. Investigation of phase equilibria in alloys of the Al-Zn-Mg-Cu-Zr-Sc system [J]. J Alloy Compd, 2004, 367: 10-16.
- [4] SENKOV O N, BHAT R B, SENKOVA S V, SCHLOZ J D. Microstructure and properties of cast ingots of Al-Zn-Mg-Cu alloys modified with Sc and Zr [J]. Metall Mater Trans A, 2005, 36: 2115-2126.
- [5] SHARMA M M, AMATEAU M F, EDEN T J. Hardening mechanisms of spray formed Al-Zn-Mg-Cu alloys with scandium and other elemental additions [J]. J Alloy Compd, 2006, 416: 135-142.
- [6] XU Guo-fu, MOU Shen-zhou, YANG Jun-jun, JIN Tou-nan, NIE Zuo-ren, YIN Zhi-min. Effect of trace rare earth element Er on Al-Zn-Mg alloy [J]. Transactions of Nonferrous Metals Society of China, 2006, 16(3): 598-603.
- [7] SENKOV O N, SHAGIEV M R, SENKOVA S V, MIRACLE D B. Precipitation of $\text{Al}_3(\text{Sc,Zr})$ particles in an Al-Zn-Mg-Cu-Sc-Zr alloy during conventional solution heat treatment and its effect on tensile properties [J]. Acta Mater, 2008, 56: 3723-3738.
- [8] SINGH V, PRASAD K S, GOKHALE A A. Effect of minor Sc additions on structure, age hardening and tensile properties of aluminium alloy AA8090 plate [J]. Scr Mater, 2004, 50: 903-908.
- [9] WU Z G, SONG M, HE Y H. Effects of Er on the microstructure and mechanical properties of an as-extruded Al-Mg alloy [J]. Mater Sci Eng A, 2009, 504: 183-187.
- [10] LI Y T, LIU Z Y, XIA Q K, LIU Y B. Grain refinement of the Al-Cu-Mg-Ag alloy with Er and Sc additions [J]. Metall Mater Trans A, 2007, 38: 2853-2858.
- [11] BAI S, LIU Z Y, LI Y T, HOU Y H, CHEN X. Microstructures and fatigue fracture behavior of an Al-Cu-Mg-Ag alloy with addition of rare earth Er [J]. Mater Sci Eng A, 2009, 527: 1806-1814.
- [12] ZHANG L G, LIU L B, HUANG G X, QI H Y, JIA B R, JIN Z P. Thermodynamic assessment of the Al-Cu-Er system [J]. CALPHAD, 2008, 32: 527-534.
- [13] CHEN X, LIU Z Y, BAI S, LI Y, LIN L H. Alloying behavior of erbium in an Al-Cu-Mg alloy [J]. J Alloy Compd, 2010, 505(1): 201-205.
- [14] ZHAO Z K, ZHOU T T, LIU P Y, CHEN C Q. Observation of formed Er phase in Al-Zn-Mg-Cu-Li alloys by TEM [J]. Rare Met Mat Eng, 2004, 33(10): 1108-1111.
- [15] MAO Jian-wei, JIN Tou-nan, XU Guo-fu, NIE Zuo-ren. As-cast microstructure of Al-Zn-Mg and Al-Zn-Mg-Cu alloys added erbium [J]. Transactions of Nonferrous Metals Society of China, 2005, 15(6): 1341-1345.
- [16] FAN X G, JIANG D M, MENG Q C, ZHONG L. The microstructural evolution of an Al-Zn-Mg-Cu alloy during homogenization [J]. Mater Lett, 2006, 60: 1475-1479.

Al-Zn-Mg-Cu-Zr-0.5Er 合金在铸态和均匀化条件下的组织

王少华¹, 孟令刚¹, 杨守杰², 房灿峰¹, 郝海¹, 戴圣龙², 张兴国¹

1. 大连理工大学 材料科学与工程学院, 大连 116024;

2. 北京航空材料研究院, 北京 100095

摘要: 采用普通半连续铸造技术(DCC)制备了 Al-Zn-Mg-Cu-Zr 和 Al-Zn-Mg-Cu-Zr-0.5Er 合金, 研究了微量元素 Er 对 Al-Zn-Mg-Cu-Zr 合金铸态和均匀化态组织的影响。结果表明: 添加 0.5%Er 后, 合金的晶粒尺寸增大且为粗大的树枝晶。在合金凝固过程中, 大部分元素 Er 在晶界处形成三元合金相 $\text{Al}_8\text{Cu}_4\text{Er}$ 。经过均匀化处理后, 两种合金晶界处的 MgZn_2 相几乎全部回溶。但是在含 Er 合金中, 由于 $\text{Al}_8\text{Cu}_4\text{Er}$ 相的回溶温度约为 575 °C, 所以均匀化处理不能有效地消除 $\text{Al}_8\text{Cu}_4\text{Er}$ 相。

关键词: Al-Zn-Mg-Cu-Zr 合金; 钪; $\text{Al}_8\text{Cu}_4\text{Er}$ 相; 均匀化; 显微组织

(Edited by YANG Hua)